

TriLock: IC Protection with Tunable Corruptibility and Resilience to SAT and Removal Attacks

Yuke Zhang¹, Yinghua Hu¹, Pierluigi Nuzzo, and Peter A. Beerel

Department of Electrical and Computer Engineering, University of Southern California, Los Angeles, CA, USA
{yukezhan, yinghuah, nuzzo, pabeerel}@usc.edu

Abstract—Sequential logic locking has been studied over the last decade as a method to protect sequential circuits from reverse engineering. However, most of the existing sequential logic locking techniques are threatened by increasingly more sophisticated SAT-based attacks, efficiently using input queries to a SAT solver to rule out incorrect keys, as well as removal attacks based on structural analysis. In this paper, we propose TriLock, a sequential logic locking method that simultaneously addresses these vulnerabilities. TriLock can achieve high, tunable functional corruptibility while still guaranteeing exponential queries to the SAT solver in a SAT-based attack. Further, it adopts a state re-encoding method to obscure the boundary between the original state registers and those inserted by the locking method, thus making it more difficult to detect and remove the locking-related components.

Index Terms—Sequential Logic Locking, SAT-Based Attacks, Hardware Security

I. INTRODUCTION

The decentralization of the integrated circuit (IC) supply chain over the past few decades has increasingly raised concerns about potential threats, such as intellectual property (IP) piracy and hardware Trojan insertion [1]. One of the most investigated IC protection schemes against these threats is logic encryption (or locking) [2]–[8], which adds programmability to the design at the gate or register-transfer level (RTL), so that the intended function is hidden from unauthorized users, and can only be accessed by a legal user by appropriately configuring the locked circuit.

Early logic locking methods have mostly focused on modifying the combinational portion of a circuit [3], [4]. On the other hand, *sequential logic locking*, the focus of this paper, usually involves creating new states in the finite state machine representing the original circuit and modifying its transitions [2], [6], [9]–[13]. The correct functionality is typically retrieved by either providing a key sequence, i.e., a dynamic sequence of key patterns, via the primary input ports during the first few clock cycles [2], [9] or by setting a set of key ports to fixed values throughout the circuit operation time [11]–[13]. Sequential locking shows the promise of significantly increasing the attack effort at reasonable cost by judiciously expanding a circuit’s state space. Yet, major threats to existing schemes have been posed by increasingly more sophisticated SAT-based attacks, efficiently using queries to a Boolean

satisfiability (SAT) solver to rule out incorrect keys, as well as removal attacks that can exploit structural circuit signatures.

SAT-based attacks [6], [14], [15], leveraging circuit unrolling and model checking, have shown to be successful against the first versions of sequential locking [2], in that they can effectively exploit the early occurrence of output errors to dramatically decrease the number of SAT queries and accelerate the key search. This vulnerability has called for methods that can intentionally postpone the first occurrence of the output errors [9]–[11], [13]. However, SAT-based attacks can still be accelerated by leveraging functional corruptibility to help estimate the required circuit unrolling depth and further reduce the number of SAT queries [16]. Moreover, SAT-resilient methods tend to exhibit poor error rates, usually captured in terms of *functional corruptibility*, hence lack enough protection – a trade-off that is extensively documented in the context of combinational locking [17], [18]. Finally, the net boundary between the locking-related components and the rest of the circuit makes them vulnerable to removal attacks [19], possibly boosted by machine learning-assisted netlist analysis tools [20], [21]. *A robust sequential locking scheme that can offer quantifiable protection and resilience to SAT-based and removal attacks is still elusive.*

This paper proposes TriLock, an IC protection scheme that leverages the temporal dimension of sequential locking to break the well-known trade-off between SAT-attack resilience and functional corruptibility of combinational locking and simultaneously address all of the above challenges. Our contributions include:

- A cost-effective logic locking method that can exponentially increase the number of SAT queries required for a successful SAT-based attack.
- An error-generation mechanism that can strategically increase the output error rate to achieve a desired functional corruptibility without compromising SAT-attack resilience.
- A state re-encoding technique that can significantly blur the boundary between the original circuit and the logic added by the locking scheme.

To the best of our knowledge, TriLock is the first sequential locking technique that simultaneously tackles all the above security objectives. We demonstrate its effectiveness via security analysis and empirical validation on ISCAS’89 [22] and ITC’99 [23] benchmarks.

¹Yuke Zhang and Yinghua Hu contributed equally to this work. This work is based on research sponsored by the U.S. Government. The views and conclusions contained herein are those of the authors and should not be interpreted as necessarily representing the official policies or endorsements of the U.S. Government.

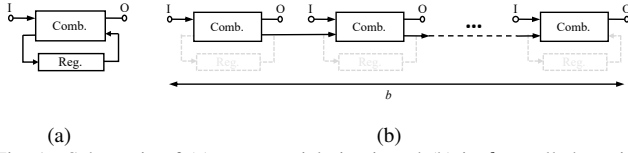


Fig. 1. Schematic of (a) a sequential circuit and (b) its b -unrolled version.

II. BACKGROUND AND RELATED WORK

We discuss SAT-based and removal attacks as well as the methods that have been proposed to counteract them.

A. Preliminaries

In the following, we just use the term circuit to refer to a sequential circuit. For a circuit C , shown in Fig. 1(a), its b -unrolled version, denoted by C_b , is a combinational circuit, shown in Fig. 1(b), that represents the behavior of C over the first b clock cycles. We denote by I and O the sets of input and output ports of C , respectively, by k and i its key and input sequence, respectively, and by κ the (cycle) length of k , i.e., the number of clock cycles required to provide k to the circuit after reset. For a sequence s , s_n denotes the sub-sequence of s associated with the n -th unrolling (clock cycle) and $s_{n \leftrightarrow m}$ the one associated with the range of unrollings from n to m .

Let C_b^o be the b -unrolled version of the original circuit and C_b^e , with a slight abuse of notation, the $(\kappa+b)$ -unrolled version of the encrypted circuit. For simplicity, we refer to C_b^e as the b -unrolled version of the encrypted circuit, by skipping the first κ cycles used to input the key. Let the functions implemented by C_b^o and C_b^e be $f_b : \mathbb{B}^{b|I|} \rightarrow \mathbb{B}^{b|O|}$ and $f'_b : \mathbb{B}^{\kappa|I|} \times \mathbb{B}^{b|I|} \rightarrow \mathbb{B}^{b|O|}$, respectively. Then, the *functional corruptibility* (FC) of a b -unrolled version of an encrypted circuit is defined as [16]

$$FC_b = \frac{1}{2^{(\kappa+b)|I|}} \sum_{i \in \mathbb{B}^{b|I|}} \sum_{k \in \mathbb{B}^{\kappa|I|}} \mathbb{1}(f_b(i) \neq f'_b(i, k)), \quad (1)$$

where $\mathbb{1}(\cdot)$ is the indicator function. FC_b quantifies the proportion of errors over all input-key combinations for a b -unrolled encrypted circuit.

B. SAT-Based Attacks

The idea of formulating a SAT problem to prune out wrong keys was first adopted by the SAT attack COMB-SAT [24] to combinational logic locking. COMB-SAT assumes that the attacker has access to the netlist of the locked circuit as well as unlimited access to the correct input/output pairs from the original circuit. An iterative key elimination process is executed by searching for distinguishing input patterns (DIPs) via SAT solving. A DIP is an input pattern of the locked circuit for which there exist two different keys that lead to different outputs. When a DIP d is found, it can effectively rule out a set of wrong keys K_d that are detectable by d , expressed as

$$K_d = \{k | f(d) \neq f'(d, k)\}, \quad (2)$$

where f and f' are the functions implemented by the original and the locked circuit, respectively. Until the correct key is obtained, more DIPs are iteratively found and used to further prune out the key search space. A trade-off exists between SAT-attack resilience, i.e., the number of DIPs required to find

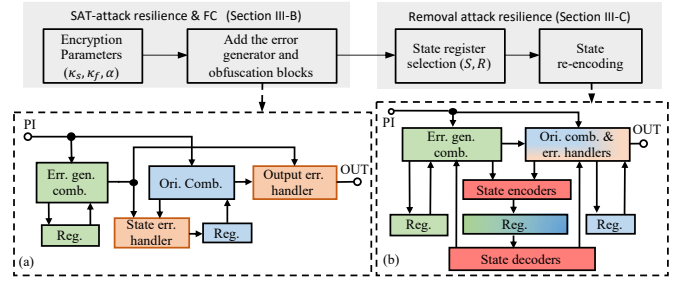


Fig. 2. Overview of TriLock.

the correct key, and the FC of a locked circuit [17], [18]. The larger the number of errors induced by a wrong key, the higher the likelihood that the wrong key can be detected and eliminated by a DIP.

COMB-SAT cannot be directly applied to sequential circuits without scan access to their internal states. It can, however, be extended by relying on circuit unrolling to generate a b -unrolled version of the encrypted circuit, C_b^e , on which to apply COMB-SAT [6], [14], [15]. Once a key is found for C_b^e , model checking is performed to verify whether the key is also correct for C^e , beyond the first b clock cycles. If this check fails, the above steps will be repeated for a larger b . Several sequential encryption methods [9]–[11], [13] boost SAT-attack resilience by increasing the minimum unrolling depth b^* that is needed to rule out all the wrong keys. However, b^* has been recently shown to be effectively predictable [16], thus making SAT-based attacks even more efficient.

C. Removal Attacks

Sequential logic encryption methods may be vulnerable to removal attacks based on structural analysis of the circuit netlist [12], [19]–[21]. Unwanted signatures may be detected in the state transition graph (STG) of the encrypted circuit, for example, when there is only one edge from the set of states added by the locking logic to the states in the original STG [2]. Graph analysis methods can then be applied to the STG to recognize the boundary between the two sets of states [19]. State-Deflection [10] adds several sink state clusters in the STG to trap illegal users. However, because a sink cluster does not have any outgoing edge, it can be easily identified by a strongly connected component (SCC) algorithm.

Several papers [20], [21] view the recognition of state registers as the first step for reverse-engineering finite state machines, and propose accurate tools for this task. After the state registers are recognized, the original registers must be separated from the additional registers associated with the encryption logic. In this paper, we assume that all the state registers of a circuit can be successfully recognized. The aim of TriLock is to make it more difficult to separate and remove the additional registers associated with the encryption.

III. TRILOCK

We first discuss the trade-off between SAT-attack resilience and FC and present in Section III-A a naive implementation of TriLock that achieves high resilience at the cost of low FC. We show how to overcome the trade-off in Section III-B,

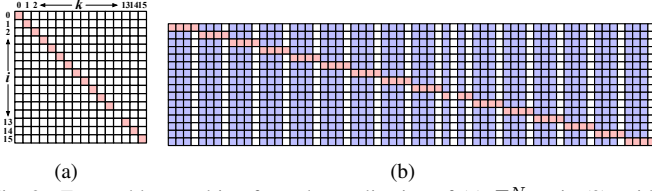


Fig. 3. Error tables resulting from the application of (a) E_b^N as in (3), with $|I| = \kappa = b^* = b = 2$ and (b) E_b^{SF} as in (16), with $|I| = \kappa_s = b^* = b = 2$ and $\kappa_f = 1$.

allowing independent configuration of FC without compromising SAT-attack resilience. We finally detail our strategy to mitigate removal attacks in Section III-C. The encryption flow of TriLock is shown in Fig. 2.

A. Trade-off Between SAT-Attack Resilience and FC

Combinational logic encryption techniques, such as SAR-Lock [4] and Anti-SAT [5], adopt point functions to achieve exponential SAT-attack resilience, quantified in terms of the required number of DIPs (n_{dip}). In these methods, each DIP can only rule out a limited number of wrong keys at each iteration of the SAT attack. We apply a similar concept in TriLock to achieve exponential n_{dip} in the key length κ . We assume that an attacker can efficiently estimate the minimum required unrolling depth b^* [16] and perform COMB-SAT directly on C_b^e , with $b \geq b^*$. We then focus on guaranteeing an exponential n_{dip} for C_b^e .

We define an *error function*, $E_b : \mathbb{B}^{|I|} \times \mathbb{B}^{\kappa|I|} \rightarrow \{1, 0\}$, for C_b^e , as a function that takes as arguments a $b|I|$ -bit input sequence i and a $\kappa|I|$ -bit key sequence k and returns 1 if and only if an error occurs at the output of C_b^e , i.e., if and only if $f_b'(k, i) \neq f_b(i)$ holds. A naive error function that achieves exponential n_{dip} can then be obtained by setting $b^* = \kappa$ and by implementing a point function, as done, for example, in SARLock [4]. We would therefore obtain

$$E_b^N(i, k) = \mathbb{1}[(k \neq k^*) \wedge (k = i_{1 \leftrightarrow \kappa})], \quad (3)$$

where k^* , the correct key sequence, is a fixed sequence of length κ . For an arbitrary wrong key k^w , there exists a set of input sequences IS_{k^w} for which E_b^N evaluates to 1, expressed as follows,

$$IS_{k^w} = \{i \in \mathbb{B}^{b|I|} | k^w = i_{1 \leftrightarrow \kappa}\}, \quad (4)$$

that is, all the input sequences having k^w as a prefix. Based on the mechanism of COMB-SAT, any input sequence in IS_{k^w} can then be selected as a DIP to rule out the wrong key k^w . However, an input sequence in IS_{k^w} cannot detect any other wrong key, that is,

$$\forall i \in IS_{k^w}, \forall k \in \mathbb{B}^{\kappa|I|} \setminus \{k^w\}, E_b(i, k) = 0. \quad (5)$$

Consequently, one DIP can only rule out one wrong key at a time and the n_{dip} will equal the number of wrong keys, i.e.,

$$n_{dip} = 2^{\kappa|I|} - 1. \quad (6)$$

The effect of E_b^N is pictorially represented by the colored error table in Fig. 3(a) for a 2-input circuit with $\kappa = b^* = b = 2$. The row and the column indexes correspond to the values of the input and the key sequences, respectively. If $E_b^N(i, k) = 1$,

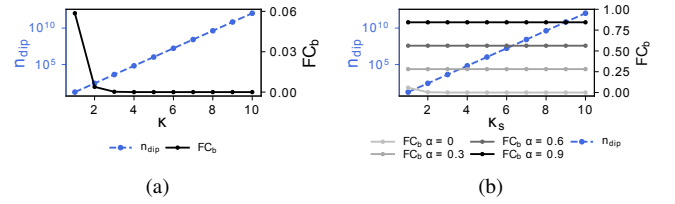


Fig. 4. Relations between n_{dip} and FC_b of a 4-input circuit implemented by (a) E_b^N , and (b) E_b^{SF} with $\kappa_f = 1$.

the corresponding square is red. By definition, FC_b can be computed as

$$FC_b = \frac{(2^{\kappa|I|} - 1) \cdot 2^{(b-\kappa)|I|}}{2^{(\kappa+b)|I|}} \approx \frac{1}{2^{\kappa|I|}} = \frac{1}{n_{dip} + 1}. \quad (7)$$

which is, unsurprisingly, low for E_b^N , as low as 0.06 in the scenario of Fig. 3(a). In the following, we detail how this trade-off between n_{dip} and FC_b , captured by (7) and pictorially shown in Fig. 4(a) for different key cycle lengths κ for a 4-input circuit, can be circumvented by appropriately designing the error function.

B. Circumventing the SAT-Attack Resilience vs. FC Trade-Off

For better clarity, we use κ_s to denote the key cycle length and rewrite the error function in (3) as follows:

$$E_b^S(i, k) = \mathbb{1}[(k \neq k^*) \wedge (k_{1 \leftrightarrow \kappa_s} = i_{1 \leftrightarrow \kappa_s})]. \quad (8)$$

We can now increase FC without compromising the attack resilience achieved by E_b^S by strategically redesigning the error function over a larger key cycle length $\kappa = \kappa_s + \kappa_f$, leading to an extended error table, as shown in Fig. 3(b) for a 2-input circuit with $\kappa_s = b^* = b = 2$ and $\kappa_f = 1$. The red squares represent the errors defined by E_b^S ; we denote their number by n_b^S , given by

$$n_b^S = (2^{\kappa|I|} - 1) \cdot 2^{(b-\kappa_s)|I|} \approx 2^{(b+\kappa_f)|I|}. \quad (9)$$

Similarly to (4), for any wrong key with prefix $k_{1 \leftrightarrow \kappa_s}^w$, there exists a set of input sequences $IS_{k^w} = \{i \in \mathbb{B}^{b|I|} | k_{1 \leftrightarrow \kappa_s}^w = i_{1 \leftrightarrow \kappa_s}\}$ that can be used as DIPs to eliminate only wrong keys with the same prefix $k_{1 \leftrightarrow \kappa_s}^w$. There are, in total, $2^{\kappa_s|I|}$ possible values for the prefix $k_{1 \leftrightarrow \kappa_s}^w$ of a wrong key, so the SAT-attack resilience corresponding to E_b^S is

$$n_{dip} = 2^{\kappa_s|I|}. \quad (10)$$

Besides the errors defined by E_b^S , we look for a set of additional input-key pairs in C_b^e such that, if an error is added at each pair, it will not decrease the SAT-attack resilience achieved by E_b^S . For a fixed sequence k^{**} of length κ_f , specified by the designer and such that $k^{**} \neq k_{(\kappa-\kappa_f) \leftrightarrow \kappa}^*$, one such set can be defined as follows:

$$P_b^{k^*, k^{**}} = \{(i, k) | k_{(\kappa-\kappa_f) \leftrightarrow \kappa} \neq k^{**} \wedge (k \neq k^*)\}, \quad (11)$$

where k^* is the correct key sequence of length κ . The blue squares in Fig. 3(b) pictorially represent $P_b^{k^*, k^{**}}$ when $k^* = 100101$ and $k^{**} = 11$. The following result states the property of $P_b^{k^*, k^{**}}$.

Theorem 1. Given two sequences k^{**} and k^* of length κ_f and κ , respectively, with $\kappa_f < \kappa$, let the b -unrolled version of the encrypted circuit C_b^e implement the error function E_b^S in (8), with $\kappa_s = \kappa - \kappa_f$. We assume that errors are inserted at all input-key pairs in $P_b^{k^*, k^{**}}$, defined as in (11), i.e., $f_b'(i, k) \neq f_b(i)$, $\forall (i, k) \in P_b^{k^*, k^{**}}$. Then, COMB-SAT on C_b^e will require at least $2^{\kappa_s |I|}$ DIPs.

Proof. Given a wrong key k^w with k^{**} as a suffix, i.e., such that $(k^w \neq k^*) \wedge (k_{(\kappa - \kappa_f)}^w \leftrightarrow \kappa = k^{**})$, by the definition of $P_b^{k^*, k^{**}}$, we have that $(i, k^w) \notin P_b$, $\forall i \in \mathbb{B}^{|I|}$. Let i^w be the DIP capable of detecting k^w . Since i^w cannot be in $P_b^{k^*, k^{**}}$, then it must satisfy $E_b^S(i^w, k^w) = 1$. Let us now assume that k^v is another wrong key with k^{**} as a suffix, and such that $k^w \neq k^v$. By (8), we conclude that $E_b^S(i^w, k^v) = 0$ holds. Therefore, the DIP that allows ruling out k^w cannot exclude any other wrong key having k^{**} as a suffix. In total, there are $2^{\kappa_s |I|}$ wrong keys with a suffix of k^{**} . Therefore, $2^{\kappa_s |I|}$ DIPs are at least required to exclude those wrong keys. \square

Theorem 1 indicates that more errors can be added to C_b^e to boost FC_b without negatively affecting the SAT-attack resilience achieved with E_b^S alone. Moreover, the number of DIPs is independent of b . We denote by n_b^{ef} the number of error-free entries on the error table. We can compute the maximum achievable FC_b as follows:

$$FC_b = \frac{2^{(\kappa+b)|I|} - n_b^{ef}}{2^{(\kappa+b)|I|}} = 1 - \frac{2^{\kappa_s |I|} \cdot 2^{b|I|}}{2^{(\kappa+b)|I|}} = 1 - \frac{1}{2^{\kappa_f |I|}}. \quad (12)$$

In the scenario of Fig. 3(b), if all the blue squares are selected as errors, FC_b can be as high as 0.75. We can select the additional errors via the following error function

$$E_b^F(i, k) = \mathbb{1} \left[(i, k) \in P_b^{k^*, k^{**}} \wedge r(i, k) \right], \quad (13)$$

where $r(i, k)$ modulates the proportion of input-key pairs in $P_b^{k^*, k^{**}}$ that are selected to place an error. In this paper, we choose

$$r(i, k) = \mathbb{1} \left[\kappa_{(\kappa - \kappa_f) \leftrightarrow \kappa} \leq \alpha (2^{\kappa_f |I|} - 1) \right], \quad (14)$$

where $\alpha \in (0, 1)$ is a design parameter used to configure the desired FC to the following value:

$$FC_b \approx \alpha \left(1 - \frac{1}{2^{\kappa_f |I|}} \right). \quad (15)$$

By combining E_b^S and E_b^F , we obtain

$$E_b^{SF}(i, k) = E_b^S(i, k) \vee E_b^F(i, k), \quad (16)$$

which is the error function adopted by TriLock to guarantee exponential SAT-attack resilience and independently configurable FC. As shown in Fig. 4(b) for a 4-input circuit with $\kappa_f = 1$, it is indeed possible to independently tune the FC_b while still keeping high SAT-attack resilience. Moreover, the n_{dip} and FC_b in (10) and (15), respectively, are independent of the unrolling depth b .

We implement the error function E_b^{SF} with the error generator block, shown in green in Fig. 2(a), whose output signals are

Algorithm 1 State register selection

Input: C^e and S .

Output: R .

```

1: RCG = create_graph(Ce); R = []; count = 0
2: E, O, M = run_scc(RCG)
3: while ((E ≠ ∅ or O ≠ ∅) and count < S) do
4:   if (E ≠ ∅ and O ≠ ∅) then
5:     SCC1, SCC2 = get_largest_scc(E, O)
6:   else
7:     temp = get_non_empty_set(E, O)
8:     SCC1, SCC2 = get_largest_scc(temp, M)
9:   end if
10:  r1, r2 = get_max_edge_node(SCC1, SCC2)
11:  R.append([r1, r2]); count = count + 1
12:  RCG = update_graph(RCG, [r1, r2])
13:  E, O, M = run_scc(RCG)
14: end while
15: return R

```

passed to the state error handler and the output error handler in orange, to trigger a signal inversion on a configurable number of state registers and primary output ports, respectively.

C. Enhancing Removal Attack Resilience: State Re-encoding

As shown in Fig. 2(a), we can distinguish the original state registers of an encrypted circuit (in blue) from the extra state registers added by the encryption (in green). Identifying the type of registers is an essential step toward removal attacks. Specifically, an attacker can leverage the SCC algorithm in a register connection graph (RCG), where a register is represented by a node and the existence of a path between two registers is denoted by a directed edge between the corresponding nodes. The output of the SCC algorithm on an RCG is one or more clusters of nodes, called SCCs. For any two nodes in the same SCC, they are reachable from each other. We denote by O-SCC, E-SCC, and M-SCC, an SCC containing only the original registers, only the extra registers, and a mix of the two types of registers, respectively.

When no SCC in an RCG is an M-SCC, the identification of the set of original or extra registers is expected to be easy, as each SCC is already a congregation of either original or extra registers. In the best case, an attacker could expect only two SCCs, an O-SCC and an E-SCC, with all the original registers and all the extra registers, respectively, as the algorithm output. Such a successful clustering of the registers would be due to the insufficient connections between original and extra registers. In contrast, if the connections are dense, one or more M-SCCs will exist and it will be harder to classify the type of registers in those M-SCCs. We then propose a *state re-encoding* method, implemented on the encrypted sequential circuit, that intentionally creates new edges between O-SCCs and E-SCCs, resulting in more registers being clustered in one or several M-SCCs. As shown in Fig. 2(b), the state re-encoding method selects a configurable number of registers, and inserts state encoders and decoders after adding the error generator and error handlers. We introduce below the register selection procedure and the encoder/decoder mechanism adopted in state re-encoding.

State Register Selection. We adopt a greedy method to iteratively select and encode pairs of original and extra reg-

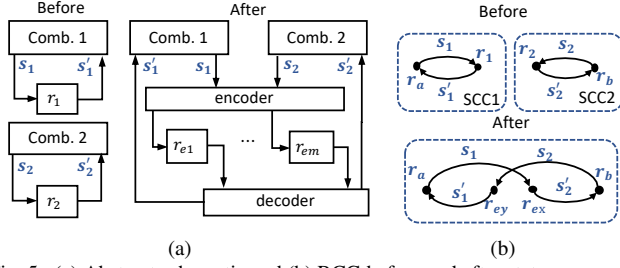


Fig. 5. (a) Abstract schematic and (b) RCG before and after state re-encoding.

isters. Algorithm 1 shows the pair selection process, which takes as inputs an encrypted netlist C^e and the desired number of register pairs S , and returns a list of register pairs R as output. After creating the RCG from C^e (line 1) and running the SCC algorithm (line 2), three sets, i.e., E , O , and M , are generated that contain all the E-SCCs, O-SCCs, and M-SCCs, respectively. To maximize the impact of state re-encoding for a single pair of original and extra registers, we first identify the largest O-SCC and E-SCC as SCC_1 and SCC_2 , respectively (line 5). In case there does not exist an E-SCC or O-SCC, we choose the largest M-SCC as the replacement (line 7-8). In SCC_1 and SCC_2 , we then select the nodes connected by the largest number of edges, denoted as r_1 and r_2 , respectively (line 10). We record (r_1, r_2) in R (line 11) and update the RCG (line 12-13) as a result of re-encoding (r_1, r_2) . The above register pair selection process is iterated until the designer-specified number of pairs is reached or no E-SCC and O-SCC exist.

Encoder/Decoder Mechanism. For each pair of registers (r_1, r_2) in R , a state encoder and a state decoder are inserted between the combinational logic and the two registers, r_1 and r_2 , as shown in Fig. 5(a), to merge the SCC containing r_1 (SCC_1) and the one containing r_2 (SCC_2). We denote by $enc(\cdot)$ and $dec(\cdot)$ the functions of the encoder and the decoder, respectively. Between the encoder and the decoder, r_1 and r_2 are replaced by a set of encoded state registers r_{ei} , where $1 \leq i \leq m$. We denote by s_1 (s_1') the net connecting from (to) the combinational logic to (from) r_1 . Similar notations are used for r_2 .

To prevent the encoder/decoder structure from affecting the circuit function, a fixed-point condition $dec(enc(a)) = a$ should hold for any 2-bit sequence a . Moreover, state re-encoding should achieve successful merging of the two SCCs into one M-SCC, which requires the existence of the following looped signal propagation path (abbreviated as a path):

$$\exists x, y \in [1, m] : s_1 \rightarrow r_{ex} \rightarrow s_2' \rightarrow s_2 \rightarrow r_{ey} \rightarrow s_1' \rightarrow s_1. \quad (17)$$

When such a looped path exists, any register r_a in SCC_1 can connect to any register r_b in SCC_2 via the path: $r_a \rightarrow s_1 \rightarrow r_{ex} \rightarrow s_2' \rightarrow r_b$, as shown in Fig. 5(b). Similarly, r_b can also reach r_a via the path: $r_b \rightarrow s_2 \rightarrow r_{ey} \rightarrow s_1' \rightarrow r_a$. On the RCG, the above paths construct a bidirectional edge between r_a and r_b , which merges SCC_1 and SCC_2 into an M-SCC.

In this paper, we implement the encoder with two arithmetic operations, namely, $e_1 = s_1 + s_2$ and $e_2 = s_1 - s_2$, where e_1 and e_2 are the encoded states. The decoder also executes two arithmetic operations, $s_1' = \frac{1}{2}(e_1 + e_2)$ and $s_2' = \frac{1}{2}(e_1 - e_2)$, which satisfies the fixed-point condition

 TABLE I
 SAT-ATTACK RESILIENCE OF TriLock

Circuit	Circuit Info.				$\kappa_s = 1$		$\kappa_s = 2$		$\kappa_s = 3$	
	PI	PO	FF	Gate	n_{dip}	T (s)	n_{dip}	T (s)	n_{dip}	T (s)
s9234	19	22	228	5597	524288	3.9e+06	2.7e+11	2.1e+12	1.4e+17	1.1e+18
s15850	13	87	597	9772	8192	105283	6.7e+07	5.0e+08	5.5e+11	4.1e+12
s35932	35	320	1728	16065	3.4e+10	2.6e+11	1.2e+21	8.8e+21	4.1e+31	3.0e+32
s38417	28	106	1636	22179	2.7e+08	2.0e+09	7.2e+16	5.4e+17	1.9e+25	1.4e+26
s38584	11	278	1452	19253	2048	27394.01	4.2e+06	3.1e+07	8.6e+09	6.4e+10
b12	5	6	121	1000	32	55.44	1024	1934.18	32768	244449.28
b14	32	54	245	8567	4.3e+09	3.2e+10	1.8e+19	1.4e+20	7.9e+28	5.9e+29
b15	36	70	447	6931	6.9e+10	5.1e+11	4.7e+21	3.5e+22	3.2e+32	2.4e+33
b18	37	23	20372	94249	1.4e+11	1.0e+12	1.9e+22	1.4e+23	2.6e+33	1.9e+34
b20	32	22	490	17158	4.3e+09	3.2e+10	1.8e+19	1.4e+20	7.9e+28	5.9e+29

while creating a looped path as in (17). The associated two SCCs are, thus, merged into an M-SCC. To mitigate the structural signature produced by repeatedly implementing the same encoder/decoder, various $enc(\cdot)$ and $dec(\cdot)$ can be applied to different register pairs, which can be subject of future work.

IV. EXPERIMENTAL RESULTS

We implement the encryption flow of TriLock in Python, using Synopsys Design Compiler and a 45nm Nangate Open Cell Library [25] as the synthesis tool and the target library, respectively. FC is simulated with 800 random inputs and keys using Synopsys VCS, while the SAT-attack resilience is evaluated via an implementation of a state-of-the-art SAT-based attack [16] which can effectively predict the minimum required unrolling depth b^* . In the case of TriLock, $b^* = \kappa_s$. We select ten benchmark circuits from ISCAS'89 [22] and ITC'99 [23], as shown in Table I. All experiments are executed on an Intel(R) Xeon(R) E5-2450 2.5-GHz CPU with 126-GB memory.

SAT-Attack Resilience. Table I shows n_{dip} and the runtime resulting from applying the attack on the selected benchmark circuits when κ_s ranges from 1 to 3, and κ_f , α and S are fixed to 1, 0.6, and 10, respectively. With a two-day time-out threshold, four experiments terminated successfully. The results show that the achieved SAT-attack resilience is consistent with (10). For the rest of the experiments, denoted in blue, we show n_{dip} as computed by (10) and extrapolate the runtime by conservatively assuming a constant ratio between the runtime and n_{dip} that can be acquired from the finished experiments. According to Table I, 76.6% of the attack experiments are expected to require more than one year to finish.

Functional Corruptibility. Fig. 7 reports the simulated FC_b for different α and κ_f . We set $\kappa_s = 4$ to achieve high SAT-attack resilience, since $\kappa_s = 3$ can already achieve high resilience for most circuits in Table I. For each locking configuration, we plot the average of the simulated FC_b for b ranging from κ_s to $\kappa_s + 5$. Our results show that FC_b is close to its estimate in (15), with an absolute error within ± 0.05 , which illustrates TriLock's ability to configure FC with high SAT-attack resilience.

Removal Attack Resilience. For each benchmark circuit, we perform state re-encoding with $S = 10$ and $S = 30$. In addition, we generate a reference design with no state re-encoding, i.e., $S = 0$. Table II shows the results of the SCC algorithm. In addition to the number of different types of

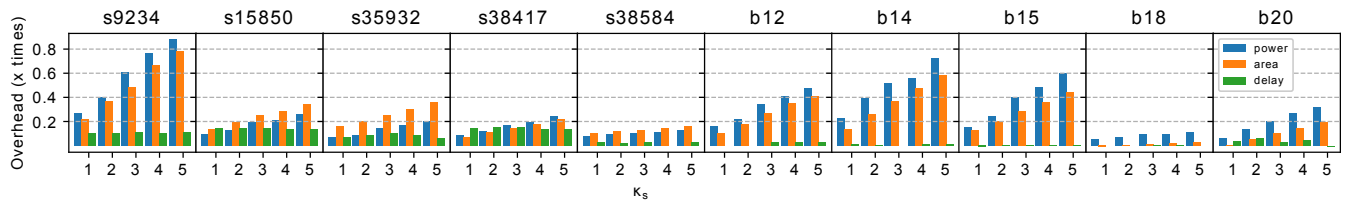


Fig. 6. Area, power, and delay overhead of TriLock with $\kappa_f = 1$, $\alpha = 0.6$, and $S = 10$.

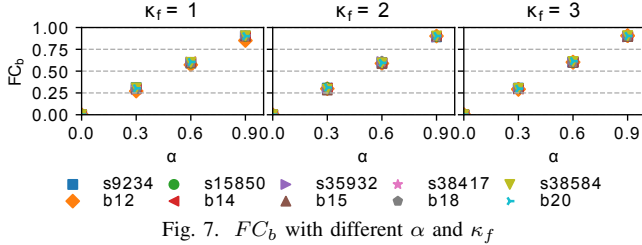


Fig. 7. FC_b with different α and κ_f

TABLE II
REMOVAL ATTACK RESILIENCE OF TRILOCK

Circuit	$S = 0$				$S = 10$				$S = 30$			
	O	E	M	P_M	O	E	M	P_M	O	E	M	P_M
s9234	72	79	0	0	12	0	1	95.2	0	0	1	100
s15850	203	93	0	0	39	0	1	94.0	14	0	1	97.9
s35932	18	317	0	0	0	0	1	100	0	0	1	100
s38417	889	198	0	0	36	0	1	97.9	20	0	1	98.9
s38584	735	79	0	0	30	0	1	97.5	0	0	1	100
b12	19	37	0	0	0	0	1	100	0	0	1	100
b14	57	226	0	0	45	0	1	90.4	24	0	1	95.1
b15	141	254	0	0	91	0	1	87.1	61	0	1	91.8
b18	95	261	0	0	53	0	1	98.4	42	0	1	98.7
b20	43	226	0	0	31	0	1	95.6	10	0	1	98.6

SCCs, denoted by O , E , and M , we show the percentage of registers that are in M-SCCs, which is denoted by P_M . On average, the numbers of O-SCCs and E-SCCs are reduced by 71.71% and 100% when 10 register pairs are selected for state re-encoding. The reduction becomes 83.80% and 100% when 30 register pairs are selected. While state re-encoding may not eliminate the existence of O-SCCs or E-SCCs for most cases in Table II, P_M being close to 100 indicates that most of the registers are clustered in one M-SCC, which means most of the original and extra registers are densely connected.

Overhead. We synthesize the locked netlists with $\kappa_f = 1$, $\alpha = 0.6$, and $S = 10$, which achieve reasonable FC and high removal attack resilience. κ_s ranges from 1 to 5 to achieve different levels of SAT-attack resilience. The overhead of area, delay, and power (ADP) is computed as percentage increase in the area, delay, and power, respectively, incurred by the locking scheme. We report the ADP overhead in Fig. 6, showing that larger circuits tend to exhibit smaller overhead. Six out of ten circuits present less than 40% in any of the ADP dimensions. In three benchmark circuits, namely, s9234, b14, and b15, the power and area overhead exceed 50% when $\kappa_s > 3$. However, as shown in Table I, these circuits can already achieve reasonably high SAT-attack resilience with $\kappa_s = 2$, where the overhead is less than 40%. In system-on-chip scenarios, it is possible to implement TriLock only on the sensitive portions of the design, making the overhead even smaller.

V. CONCLUSIONS

In this paper, we propose a cost-effective sequential logic locking technique, TriLock, to achieve both high SAT-attack resilience and high functional corruptibility, which circumvents, for the first time, the trade-off between the two security concerns that exists in combinational locking. We also present a state re-encoding technique that can significantly improve the removal attack resilience of TriLock and, potentially, other sequential locking techniques. Future work includes investigating other attack vectors [26], e.g., signature analysis on the STG, to further improve the robustness of TriLock.

REFERENCES

- [1] M. Tehranipoor *et al.*, "A survey of hardware trojan taxonomy and detection," *IEEE Design & Test of Comput.*, vol. 27, no. 1, pp. 10–25, 2010.
- [2] R. S. Chakraborty *et al.*, "HARPOON: An obfuscation-based SoC design methodology for hardware protection," *IEEE Trans. Comput.-Aided Design of Integrated Circ. and Syst.*, vol. 28, no. 10, pp. 1493–1502, 2009.
- [3] J. Rajendran *et al.*, "Fault analysis-based logic encryption," *IEEE Trans. Computers*, vol. 64, no. 2, pp. 410–424, 2013.
- [4] M. Yasin *et al.*, "SARLock: SAT attack resistant logic locking," in *IEEE Int. Symp. Hardw. Oriented Secur. and Trust (HOST)*, pp. 236–241, 2016.
- [5] Y. Xie *et al.*, "Anti-SAT: Mitigating sat attack on logic locking," *IEEE Trans. on Computer-Aided Design of Integrated Circuits and Systems*, vol. 38, no. 2, pp. 199–207, 2018.
- [6] Y. Hu *et al.*, "SANS-Crypt: Sporadic-authentication-based sequential logic encryption," in *VLSI-SoC: Design Trends* (A. Calimera *et al.*, eds.), (Cham), pp. 255–278, Springer International Publishing, 2021.
- [7] C. Pilato, A. B. Chowdhury, D. Sciuto, S. Garg, and R. Karri, "ASSURE: RTL locking against an untrusted foundry," *IEEE Transactions on Very Large Scale Integration (VLSI) Systems*, 2021.
- [8] S. D. Chowdhury *et al.*, "Enhancing SAT-attack resiliency and cost-effectiveness of reconfigurable-logic-based circuit obfuscation," in *Int. Symp. Circuits and Systems (ISCAS)*, pp. 1–5, IEEE, 2021.
- [9] A. Desai *et al.*, "Interlocking obfuscation for anti-tamper hardware," in *Proc. Cyber Secur. and Info. Intell. Research Workshop*, pp. 1–4, 2013.
- [10] J. Dofe *et al.*, "Novel dynamic state-deflection method for gate-level design obfuscation," *IEEE Trans. Comput.-Aided Design of Integrated Circ. and Syst.*, vol. 37, no. 2, pp. 273–285, 2018.
- [11] Y. Kasarabada *et al.*, "Deep state encryption for sequential logic circuits," in *IEEE Comput. Society Annual Symp. VLSI*, pp. 338–343, 2019.
- [12] S. Roshanisefat *et al.*, "DFSSD: Deep faults and shallow state duality, a provably strong obfuscation solution for circuits with restricted access to scan chain," in *IEEE VLSI Test Symp.*, pp. 1–6, 2020.
- [13] A. Rezaei *et al.*, "Sequential logic encryption against model checking attack," in *Design, Auto. and Test in Europe Conf. and Exhi.*, pp. 1178–1181, 2021.
- [14] M. El Massad *et al.*, "Reverse engineering camouflaged sequential circuits without scan access," in *2017 IEEE/ACM Int. Conf. on Comput.-Aided Design*, pp. 33–40, 2017.
- [15] K. Shamsi *et al.*, "KC2: Key-condition crunching for fast sequential circuit deobfuscation," in *Design, Auto. and Test in Europe Conf. and Exhi.*, pp. 534–539, 2019.
- [16] Y. Hu *et al.*, "Fun-SAT: Functional corruptibility-guided SAT-based attack on sequential logic encryption," *arXiv preprint:2108.04892*, 2021.
- [17] Y. Hu *et al.*, "Security-driven metrics and models for efficient evaluation of logic encryption schemes," in *ACM-IEEE MEMOCODE*, pp. 1–5, 2019.
- [18] Y. Hu *et al.*, "Risk-aware cost-effective design methodology for integrated circuit locking," in *Design, Automation and Test in Europe Conference and Exhibition (DATE)*, pp. 1182–1185, IEEE, 2021.
- [19] T. Meade *et al.*, "Revisit sequential logic obfuscation: Attacks and defenses," in *IEEE Int. Symp. Circuits and Systems*, pp. 1–4, 2017.
- [20] T. Meade *et al.*, "Gate-level netlist reverse engineering for hardware security: Control logic register identification," in *IEEE Int. Symp. Circuits and Systems (ISCAS)*, pp. 1334–1337, 2016.
- [21] J. Geist *et al.*, "RELIC-FUN: Logic identification through functional signal comparisons," in *Proc. Design Auto. Conf.*, pp. 1–6, 2020.
- [22] F. Brglez *et al.*, "Combinational profiles of sequential benchmark circuits," in *IEEE Int. Symp. Circ. and Syst.*, pp. 1929–1934, 1989.
- [23] F. Corno *et al.*, "RT-level ITC'99 benchmarks and first ATPG results," *Design & Test of computers*, vol. 17, no. 3, pp. 44–53, 2000.
- [24] P. Subramanyan *et al.*, "Evaluating the security of logic encryption algorithms," in *IEEE Int. Symp. Hardw. Oriented Secur. and Trust*, pp. 137–143, 2015.
- [25] Silvaco, "45nm open cell library," 2019.
- [26] S. Engels *et al.*, "The end of logic locking? A critical view on the security of logic locking," *Cryptology ePrint Archive, Report 2019/796*, 2019.